Peak loops untying the degeneracy of the neutrino parameters

Masafumi Koike[1,*] and Masako Saito[1,†]

[1] *Physics Department, Saitama University, 255 Shimo-Okubo, Sakura-ku, Saitama, Saitama 338-8570, Japan*

(Dated: July 13, 2009)

Systematic analysis of the determination of the value of leptonic CP-violating angle δ and the neutrino mass hierarchy $\mathrm{sgn}\,\delta m^2_{31}$ by long baseline neutrino oscillation experiments is presented. We note the difficulty to distinguish a pair of oscillation probability spectra that are peaked at the same energy and have the same probability at that energy. We thereby set forth the peak-matching condition as a criterion of the presence of degeneracy, and visualize it by intersections of the trajectories drawn by a peak of an oscillation spectrum while the value of δ is varied from 0 to 2π. We numerically calculate the pairs of the trajectories for both hierarchies and show that the pair becomes disjoint as the baseline gets longer than a critical length, indicating the matter effect resolving the degeneracy on the hierarchy. We formulate the trajectories into analytic expressions and evaluate the critical length. We provide prospects of the following four approaches of resolving the hierarchy: making the baseline longer than the critical length, using both neutrinos and anti-neutrinos, combining experiments with different baseline lengths, and observing two or more oscillation peaks.

PACS numbers: 14.60.Pq, 11.30.Er, 13.15.+g, 14.60.Lm

I. INTRODUCTION

The knowledge of the flavor structure of the lepton sector has been vastly improved through the accumulation of experimental studies on the neutrino oscillation [1], yet it is still incomplete; in the parametrization of reference [2], the values of a mixing angle θ_{13}, the mass hierarchy $\mathrm{sgn}\,\delta m^2_{31}$, and the CP-violating angle δ are still poorly known. No lower bound of θ_{13} is given at present and the values of $\mathrm{sgn}\,\delta m^2_{31}$ and δ are not known at all. The leptonic CP-violation search is one of the most exciting goal the neutrino experiments can offer. It is done by observing the appearance channel such as $\nu_\mu \to \nu_\mathrm{e}$, which is suppressed by a small factor of $\sin^2 2\theta_{13}$. On this account, we expect the two-staged strategy in the search for CP violation: the first stage is the search for θ_{13} using nuclear reactors [3] and accelerators [4], which currently targets the sensitivity of $\sin^2 2\theta_{13} \sim O(10^{-2})$; the second stage is the search for the sign of δm^2_{31} and for the CP violation, for which the next generations of long baseline neutrino oscillation experiments will offer promising opportunities [4].

We focus upon the second stage, expecting the discovery of sufficiently large value of θ_{13} in the first stage. We consider the search for the CP-violating angle through long baseline neutrino oscillation experiments using a conventional beam of muon neutrinos. The search for δ and $\mathrm{sgn}\,\delta m^2_{31}$ are mutually entangled and the values of these two are not necessarily determined uniquely by a single experiment with a fixed baseline length, leaving a degeneracy of parameter values. The parameter degeneracy obstructs the search for the parameter values and should be avoided [5, 6, 7, 8, 9]. We introduce an intuitive illustration on the determination of the parameters from the oscillation spectrum, and offer a view on the emergence of degeneracy and its resolution. We note that two oscillation spectra are difficult to distinguish and likely to cause the degeneracy when they are peaked at the same energy and the oscillation probabilities at the peak coincide. We trace the oscillation peak varying the values of δ and $\mathrm{sgn}\,\delta m^2_{31}$ to show how the search for them is entangled and the degeneracy is invited. We change the baseline length as well and illustrate from our point of view how the degeneracy disappears when the baseline gets long. We organize these analyses by deriving analytic expressions of the oscillation probability at the peaks and offer an outlook of the presence of degeneracy and possible ways to avoid it.

The outline of this paper is as follows. In Sec. II, we present the peak-matching condition as a criterion for the presence of degeneracy and show an organized view of the emergence of the degeneracy. In Sec. III, we derive an analytic expression for the $\nu_\mu \to \nu_\mathrm{e}$ appearance probability at their peaks to show how the loops move and change the shape in varying the baseline length. In Sec. IV, we apply the peak loops to the evaluation of four methods to avoid the degeneracy. Section V presents the conclusion and discussions.

*Electronic address: koike@krishna.th.phy.saitama-u.ac.jp
†Electronic address: msaito@krishna.th.phy.saitama-u.ac.jp

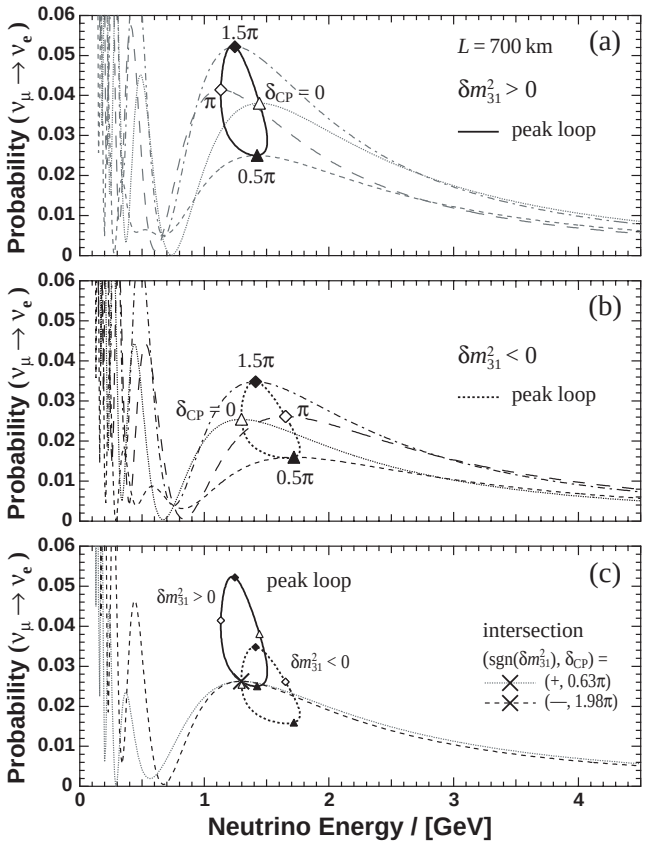

FIG. 1: The $\nu_\mu \to \nu_e$ appearance probabilities and the trajectories of their first peaks for the baseline length of 700 km. The oscillation parameters in Eq. (1) are adopted. The top figure (a) is for the normal hierarchy and the middle (b) for the inverted, and each includes the probability spectra for $\delta = 0, \pi/2, \pi$ and $3\pi/2$. The bottom figure (c) reproduces the trajectories in (a) and (b) overlaid, along with two oscillation spectra peaked at the crossed intersection of these trajectories.

II. PEAK-MATCHING CONDITION AND PRESENCE OF DEGENERACY

We assume that the number of neutrino generations is three and use the standard definitions of the quadratic mass differences δm^2_{ij} ($\{i,j\} \subset \{1,2,3\}$), the mixing angles θ_{ij}, and the CP-violating angle δ [2]. We consider a search for the value of δ and the mass hierarchy $\mathrm{sgn}\,\delta m^2_{31}$ by observing $\nu_\mu \to \nu_e$ appearance probability in long baseline neutrino oscillation experiments. Let us illustrate with an example that $\nu_\mu \to \nu_e$ appearance probability enables us to pursue the sign of δm^2_{31} and the value of δ. We show in Fig. 1 the $\nu_\mu \to \nu_e$ appearance probabilities for baseline length $L = 700\,\mathrm{km}$. The value of δ and the sign of δm^2_{31} are varied while other parameters are fixed to the following set of example values allowed by the experimental limits [2]:

$$\begin{aligned} &\delta m^2_{21} = 8.2 \times 10^{-5}\,\mathrm{eV}^2\,,\ \left|\delta m^2_{31}\right| = 2.5 \times 10^{-3}\,\mathrm{eV}^2\,, \\ &\sin^2 2\theta_{12} = 0.84\,,\ \sin^2 2\theta_{23} = 1.0\,,\ \sin^2 2\theta_{13} = 0.06\,. \end{aligned} \tag{1a}$$

The matter density ρ on the baseline is assumed to be constant and take a reference value of

$$\rho = 2.6\,\mathrm{g/cm}^3, \tag{1b}$$

which is related to the electron number density on the matter n_e as $n_e = N_A Y_e \rho$ with the Avogadro constant N_A and the proton-to-nucleon ratio Y_e on the baseline. We take the values of Eq. (1) with $Y_e = 0.5$ in our following numerical calculations unless otherwise noticed. Figure 1 shows the energy spectra of appearance probability (a) for $\delta m^2_{31} > 0$ (normal hierarchy) and (b) for $\delta m^2_{31} < 0$ (inverted hierarchy). Figure 1 (c) shows the probability for the parameter values given in the figure. We can clearly see in (a) and (b) the dependence of appearance probability upon $\mathrm{sgn}\,\delta m^2_{31}$ and δ enables the search for these parameters through ν_e appearance experiments.

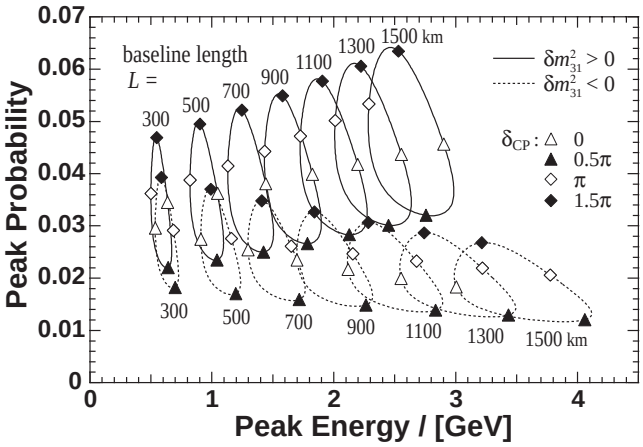

FIG. 2: Trajectories of the first oscillation peak for the baseline lengths between 300 km and 1500 km. The oscillation parameters in Eq. (1) are adopted. The solid line is for the normal hierarchy and the dotted one for the inverted.

In spite of this dependence, experiments may allow parameter values in more than one regions of parameter space and leave them with degeneracy, which should be resolved [5, 6, 7, 8, 9]. The insight to the presence of degeneracy is enlightening for this purpose, yet is difficult to gain due to complicated dependence of experimental results on many oscillation parameters and controllable setups. Searching for a succinct criterion of its presence, we focus on the peak of the oscillation probability spectrum. The two spectra in Fig. 1 (c), having the position of oscillation peaks in the E-P plane in common at the cross, show a notable similarity of the shapes over the energy range above about 1 GeV, and are expected to be difficult to distinguish by experiments with the typical visible energy $E > (0.5-1.0)$ GeV of neutrinos. This expectation can be confirmed by the χ^2 goodness-of-fit analyses [10]. We put the above observation into the following statement of the peak-matching condition as a criterion of the presence of the degeneracy [9]. Let us denote the peaks of the appearance probability spectrum by (E_n, P_n) $(n = 0, 1, 2, \cdots)$ with $E_0 > E_1 > E_2 > \cdots$, and suppose that the visible energy includes only one of them. The two sets of parameter values, collectively denoted by $\{\vartheta_i\}$ and $\{\vartheta'_i\}$, are expected to be degenerate degenerate when the peak-matching condition

$$E_n\big(\{\vartheta_i\}\big) = E_n\big(\{\vartheta'_i\}\big)\,, \tag{2a}$$

$$P_n\big(\{\vartheta_i\}\big) = P_n\big(\{\vartheta'_i\}\big) \tag{2b}$$

is satisfied by this visible peak.

We visualize this condition by introducing a trajectory made by an oscillation peak as the value of δ varied from 0 to 2π while other parameters kept fixed. The position of a peak for the normal (inverted) hierarchy moves clockwise (counterclockwise) as the value of δ increases. A trajectory of a peak forms a closed loop as presented in Fig. 1 (a) and (b) for the first peak ($n = 0$) of respective hierarchies, and intersects with the loop for the other hierarchy as seen in Fig. 1 (c), where one of them are marked by a cross. The parameter values corresponding to the intersections are the ones that satisfy the peak-matching condition. In the example of Fig. 1 (c), the pairs of the values of $(\mathrm{sgn}\,\delta m^2_{31}, \delta)$ that give the intersections are

$$\big\{(+, 0.63\pi)\,, (-, 1.98\pi)\big\}\,, \quad \big\{(+, 0.12\pi)\,, (-, 1.34\pi)\big\}\,. \tag{3}$$

If the true set of parameter values is one of the above along with Eq. (1a), the experiments would leave the degeneracy with the other of the peak-matching pair. The parameter values corresponding to the paralleling sides of the loops would be also degenerate, especially when these sides are indistinguishable due to the limited experimental resolution.

Equipped by the peak loops, we apply them to examine how the degeneracy emerges and disappears as we vary the baseline length of the neutrino oscillation experiments. We present in Fig. 2 peak loops for baseline length from 300 km to 1500 km. For a relatively short baseline ($L \sim 300$km for our example), the loop for the normal hierarchy ("normal loop") and for the inverted hierarchy ("inverted loop") have similar shape and lie significantly overlapped with each other. As a baseline gets longer, the normal loop and the inverted loop move right-upward and left-downward, respectively, and diverge due to the matter effect. The normal loop is expanded in the E- and the P-direction, while the inverted loop is appreciably stretched in the E-direction and flattened in the P-direction. The pair of loops becomes disjoint at a critical length $L_{\rm crit}$, which is in between $1100-1300$ km in this example as seen in Fig. 2.

The study so far leads us to the following outlooks upon determining the CP-violating angle and the mass hierarchy. In a short baseline length, the pair of loops overlaps considerably and consequently the hierarchy is difficult to determine by experiments. The search for δ in this case is entangled with that for the hierarchy, and its value is also difficult to determine. Another obstacle is invited by the limitation on the energy resolution which may not be enough to distinguish the paralleling sides of the narrow loops. As the baseline gets longer, the pair of loops becomes separated and the determination of the hierarchy is made easier. The search for the CP-violating angle becomes disentangled from the hierarchy search at the same time. The flattened shape of the inverted loops for a long baseline gives rise to the requirement on precise and accurate measurements of the oscillation probability to avoid introducing an extra degeneracy.

III. ANALYTIC STUDY OF THE PEAK LOOPS

In this section, we derive an analytic expression of the oscillation probability to formulate properties of the peak loops [9]. We thereby show how a pair of peak loops for $\delta m^2_{31} \gtrless 0$ distort and are separated as the baseline length increases.

We derive a formula of the oscillation probability by treating $\Delta_{21} \equiv \delta m^2_{21} L/2E$ and $\Delta_{\rm m} \equiv \sqrt{2} G_{\rm F} n_{\rm e} L = \sqrt{2} G_{\rm F} N_{\rm A} Y_{\rm e} \rho L$ as perturbation parameters, where $G_{\rm F}$ is the Fermi constant, and expand the S-matrix systematically [11]. We calculate the $\nu_\mu \to \nu_{\rm e}$ appearance probability to the second order to investigate the distortion of the peak loops in varying the baseline length. The result turns out to be lengthy, and we apply an additional approximation considering the smallness of θ_{13} and the relation $\Delta_{\rm m} > \Delta_{21}$, which holds for the cases we are interested in: we drop $O(\sin^2\theta_{13})$-terms in the coefficients of Δ^2_{21} and $\Delta_{\rm m}\Delta_{21}$ as well as $O(\sin^3\theta_{13})$-terms in that of $\Delta^2_{\rm m}$. We then obtain

$$P(\nu_\mu \to \nu_{\rm e}, E) = 4l(A \sin^2\Theta + B)\,, \tag{4a}$$

where

$$\begin{aligned} A \;=\; & 1 + 2\frac{\Delta_{\rm m}}{\Delta_{31}}(1-2s^2_{13}) - \Delta_{21}\frac{j}{l}\sin\delta + 3\frac{\Delta^2_{\rm m}}{\Delta^2_{31}} \\ & -\Delta_{21}\frac{\Delta_{\rm m}}{\Delta_{31}}\frac{j}{l}\Big(\sin\delta + \frac{\Delta_{31}}{2}\cos\delta\Big) + \frac{\Delta^2_{21}}{2}\frac{j}{l}\bigg[\frac{j}{l}\cos\delta + (1-2s^2_{12})\bigg]\cos\delta\,, \end{aligned} \tag{4b}$$

$$\begin{aligned} \Theta \;=\; & \frac{\Delta_{31}}{2} - \frac{\Delta_{\rm m}}{2}(1-2s^2_{13}) + \frac{\Delta_{21}}{2}\Big(\frac{j}{l}\cos\delta - s^2_{12}\Big) \\ & -\frac{\Delta_{21}}{2}\frac{\Delta_{\rm m}}{\Delta_{31}}\frac{j}{l}\Big(\cos\delta + \frac{\Delta_{31}}{2}\sin\delta\Big) + \frac{\Delta^2_{21}}{2}\frac{j}{l}\bigg[\frac{j}{l}\cos\delta + \frac{1}{2}(1-2s^2_{12})\bigg]\sin\delta\,, \end{aligned} \tag{4c}$$

and

$$B = \frac{\Delta^2_{21}}{4}\frac{j^2}{l^2}\sin^2\delta\,, \tag{4d}$$

with $l = c^2_{13}s^2_{13}s^2_{23}$, $j = c^2_{13}s_{13}c_{23}s_{23}c_{12}s_{12}$, $\Delta_{ij} = \delta m^2_{ij}L/2E$, $s_{ij} = \sin\theta_{ij}$, and $c_{ij} = \cos\theta_{ij}$. The approximation employed is suitable especially for a short baseline, typically for $L < O(10^3\,{\rm km})$, and is valid at least marginally for our purpose.

We calculate the maximum of the oscillation probability of Eq. (4) and obtain the energy at the peak as

$$\begin{aligned} E_n = \frac{|\delta m^2_{31}|L}{2\Pi}\;\Bigg\{\;& \bigg[1 \mp \Delta_{\rm m}\frac{1}{\Pi}\Big(1-\frac{4}{\Pi^2}\Big)(1-2s^2_{13}) \mp Rs^2_{12} \\ & \qquad +\Delta^2_{\rm m}\frac{1}{\Pi^2}\Big(1-\frac{12}{\Pi^2}+\frac{48}{\Pi^4}\Big) - R^2\frac{1}{2}\Big(1-\frac{4}{\Pi^2}\Big)\frac{j^2}{l^2}\bigg] \\ & + R\bigg[\pm 1 - \Delta_{\rm m}\frac{1}{\Pi}\Big(1-\frac{8}{\Pi^2}\Big) - 2R(1-2s^2_{12})\bigg]\frac{j}{l}\cos\delta \\ & + R\frac{2}{\Pi}\bigg[1 \mp \Delta_{\rm m}\frac{\Pi}{4}\Big(1+\frac{8}{\Pi^2}-\frac{64}{\Pi^4}\Big) \pm R\frac{\Pi^2}{4}(1-2s^2_{12})\bigg]\frac{j}{l}\sin\delta \\ & - R^2\frac{3}{2}\Big(1+\frac{4}{3}\frac{1}{\Pi^2}\Big)\frac{j^2}{l^2}\cos 2\delta \pm R^2\frac{\Pi}{2}\frac{j^2}{l^2}\sin 2\delta\Bigg\}\,, \end{aligned} \tag{5}$$

where $n = 0, 1, 2, \cdots$ is the peak index, $\Pi \equiv (2n+1)\pi$, $R \equiv \delta m^2_{21}/|\delta m^2_{31}|$, and the top of the double sign is for $\delta m^2_{31} > 0$ and the bottom for $\delta m^2_{31} < 0$. The oscillation probability at the peak is then given by

$$\begin{aligned} P_n = 4l \ \Bigg\{ & \ \left[1 \pm \Delta_{\rm m}\frac{2}{\Pi}(1-2s^2_{13}) + R^2\frac{3}{8}\Pi^2\Big(1+\frac{4}{3}\frac{1}{\Pi^2}\Big)\frac{j^2}{l^2} + \Delta^2_{\rm m}\frac{1}{\Pi^2}\Big(1+\frac{4}{\Pi^2}\Big)\right] \\ & - \ R\frac{\Pi^2}{2}\left[\Delta_{\rm m}\frac{1}{\Pi}\Big(1-\frac{4}{\Pi^2}\Big) - R(1-2s^2_{12})\right]\frac{j}{l}\cos\delta \\ & - \ R\Pi\left[1 \pm \Delta_{\rm m}\frac{2}{\Pi}\Big(1-\frac{2}{\Pi^2}\Big) \pm Rs^2_{12}\right]\frac{j}{l}\sin\delta \\ & + \ R^2\frac{\Pi^2}{8}\Big(1-\frac{4}{\Pi^2}\Big)\frac{j^2}{l^2}\cos 2\delta \pm R^2\frac{\Pi}{2}\frac{j^2}{l^2}\sin 2\delta \Bigg\}. \end{aligned} \tag{6}$$

The peak loops for $n = 0$ is obtained by keeping track of (E_n, P_n) as the value of δ is varied over a cycle from 0 to 2π while other parameters are fixed.

Taking another step ahead, we use these expressions to formulate properties of the peak loop and their dependence on the oscillation parameters and the baseline length. We define the central position of the peak loop by the average values of E_n and P_n over a cycle of δ. It is obtained by picking the terms independent of δ in Eqs. (5) and (6), and is given up to the first order by

$$\begin{aligned} & (\overline{E}_n, \overline{P}_n) = \\ & \left(\frac{|\delta m^2_{31}|L}{2\Pi}\Big[1 \mp \frac{\Delta_{\rm m}}{\Pi}\Big(1-\frac{4}{\Pi^2}\Big)(1-2s^2_{13}) \mp Rs^2_{12}\Big], 4l\Big[1 \pm \frac{2\Delta_{\rm m}}{\Pi}(1-2s^2_{13})\Big]\right), \end{aligned} \tag{7}$$

where the double sign should be understood as in Eqs. (5) and (6). The overall factor of $\overline{E}_n$ is proportional to the baseline length and consequently drives the loop to the rightward in the E-P plane as the baseline gets longer. The subleading matter-effect term is also proportional to the baseline length, shifting the normal loop left-upward and the inverted one right-downward. These features are indeed seen in Fig. 2.

The width ΔE_n and the height ΔP_n of a loop are estimated by taking the difference of the maximum and minimum values of E_n and P_n, and are obtained up to the second order as

$$\Delta E_n = |\delta m^2_{31}|LR\frac{1}{\Pi}\sqrt{1+\frac{4}{\Pi^2}}\frac{j}{l}\left[1 \mp \Delta_{\rm m}\frac{2}{\Pi}\frac{1-32/\Pi^4}{1+4/\Pi^2} \mp R\frac{1-2s^2_{12}}{1+4/\Pi^2}\right], \tag{8a}$$

$$\Delta P_n = 8R\Pi j\left[1 \pm \Delta_{\rm m}\frac{2}{\Pi}\Big(1-\frac{2}{\Pi^2}\Big) \pm Rs^2_{12}\right]. \tag{8b}$$

The overall factor of ΔE_n widens the loop due to its proportionality to the baseline length, and the matter effect offsets the widening for the normal hierarchy and enhances it for the inverted. The dependence of ΔP_n is supplied by the matter-effect term, which heightens the normal loop and flattens the inverted one. These behaviors of the loops are also observed in Fig. 2.

The critical baseline length can also be analyzed by the peak loops. It is defined as the maximum length that keeps the intersection of the normal and the inverted loops, and is calculated in the first-order approximation as

$$\begin{aligned} L_{\rm crit} \ = \ & \frac{1}{\sqrt{2}G_{\rm F}n_{\rm e}}R\frac{\Pi}{1-12\Pi^{-2}+64\Pi^{-4}}\frac{c_{23}c_{12}s_{12}}{s_{13}s_{23}}\frac{1}{1-2s^2_{13}} \\ & \times\left[\sqrt{1-\frac{12}{\Pi^2}+\frac{64}{\Pi^4}-\frac{4}{\Pi^2}\Big(\frac{s_{13}s_{23}s_{12}}{c_{23}c_{12}}\Big)^2} - \Big(1-\frac{8}{\Pi^2}\Big)\frac{s_{13}s_{23}s_{12}}{c_{23}c_{12}}\right]. \end{aligned} \tag{9}$$

The critical length is inversely proportional to $\sin\theta_{13}$ owing to the factor $c_{23}c_{12}s_{12}/s_{13}s_{23}$, with the small correction of $O(\theta_{13})$. This length can be indefinitely long since the lower bound on the value of $\sin\theta_{13}$ is still unknown. Figure 3 shows the critical length as a function of $\sin^2 2\theta_{13}$ for the first peak, where other parameters are fixed to the example values of Eq. (1). This graph reads $L_{\rm crit} = 1150\,{\rm km}$ for $\sin^2 2\theta_{13} = 0.06$. These results are qualitatively consistent with the result presented in the reference [8].

IV. PROSPECTS OF RESOLVING THE DEGENERACY THROUGH THE PEAK LOOPS

We consider possible methods to escape from the hierarchy degeneracy in the long baseline experiments [9].

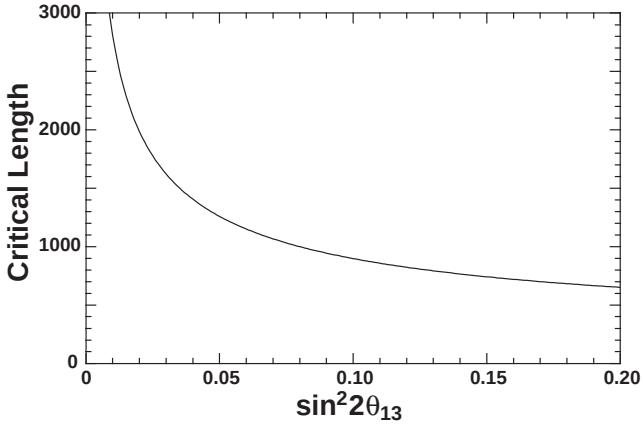

FIG. 3: The dependence of the critical length on $\sin^2 2\theta_{13}$ calculated by the first-order approximation formula of Eq. (9). The oscillation parameters in Eq. (1) are adopted except for the value of θ_{13}.

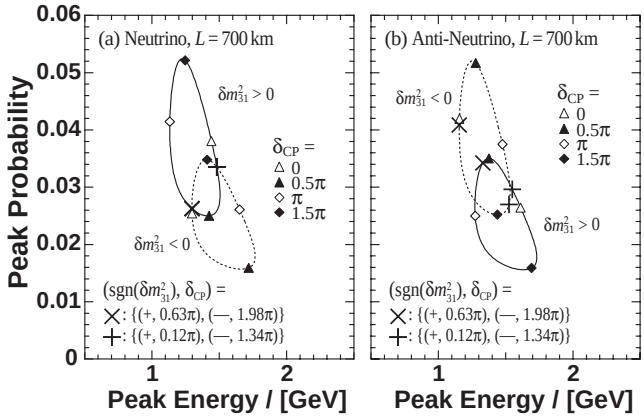

FIG. 4: Trajectories of the first peak of (a) $\nu_\mu \to \nu_e$ probability and (b) $\bar{\nu}_\mu \to \bar{\nu}_e$ probability for the baseline length of 700 km. The solid and dotted lines are for the normal and inverted hierarchy, respectively. The cross and the plus sign in (a) are on the intersections of the peak loops, and the corresponding values of parameters are also shown. The signs in (b) mark the points corresponding to these parameter values.

An experiment with baseline length longer than the critical length is a promising for this purpose, being free from the hierarchy degeneracy. Nonetheless the very long baseline also brings on the challenge such as small flux of the neutrino beam and possible large ambiguity of matter effects.

Experiments with shorter baseline are more feasible, but leaves the possibility of degeneracy. Combining the observations of two or more peaks in the search avails against this problem. We consider the following three approaches and examine them in order[1]: (2) observing $\bar{\nu}_\mu \to \bar{\nu}_e$ appearance events in addition to $\nu_\mu \to \nu_e$ events; (3) doing two or more experiments with different baseline lengths; and (4) doing an experiment that can observe two or more oscillation peaks.

The second approach employs both neutrinos and anti-neutrinos. We present in Fig. 4 two pairs of peak loops, one (a) for neutrinos and the other (b) for anti-neutrinos, with the parameter values of Eq. (1) and $L = 700$ km. Marked by a cross and a plus sign in Fig. 4 (a) are the two intersections of the normal and inverted loops. Each intersection corresponds to the hierarchy degeneracy through two sets of $(\mathrm{sgn}\,\delta m^2_{31}, \delta)$. Turning to the loop for anti-neutrinos, these sets of parameters no longer correspond to intersections but to two distinct points on the peak loops of anti-neutrinos, as shown in Fig. 4 (b) with the corresponding marks. The combined analysis of $\nu_\mu \to \nu_e$ events and

[1] Enumeration starts from (2), reserving (1) for the approach employing the baseline longer than the critical length described above.

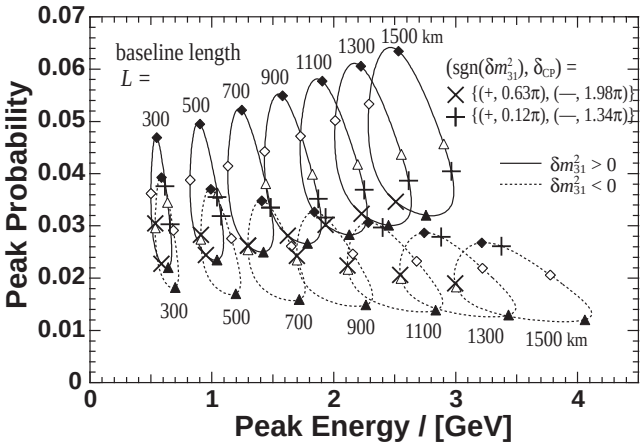

FIG. 5: The points correspond to the two sets of parameter values shown in Fig. 4, plotted on top of a series of loops reproduced from Fig. 2. Crosses and plus signs correspond to two intersections of the loops for $L = 700\,\mathrm{km}$. The oscillation parameters in Eq. (1) are adopted. The solid (dotted) line is for the normal (inverted) hierarchy.

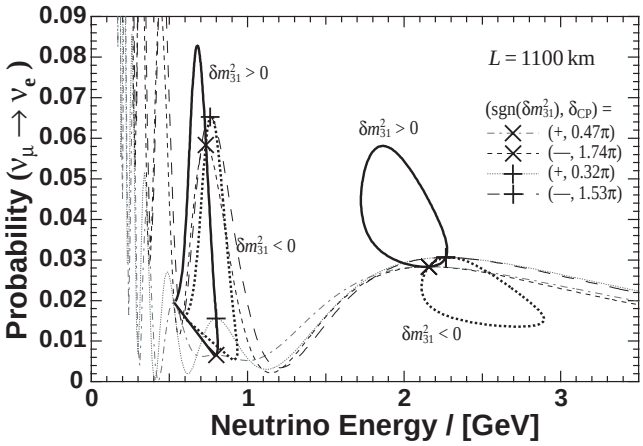

FIG. 6: Trajectories of the first and the second oscillation peak for $L = 1100\,\mathrm{km}$. The oscillation parameters in Eq. (1) are adopted. The solid (dotted) loop is for the normal (inverted) hierarchy. Crosses and plus signs correspond to the sets of parameter values that bring the first peak at the intersection of its trajectories. The points for these values are also on the second peak loops and marked by the corresponding sign. Oscillation spectra for the parameter values are overlaid.

$\bar{\nu}_\mu \to \bar{\nu}_\mathrm{e}$ events therefore helps resolve the hierarchy degeneracy. The two plus signs for anti-neutrinos are close to each other on the E-P plane in our present example, and the resolution needs to be high enough to distinguish the two points in order to make full use of the anti-neutrino channel in resolving the degeneracy.

The third approach makes use of two or more different baseline lengths [6]. We reproduce in Fig. 5 a series of peak loops shown in Fig. 2. On top of them, we mark the points correspond to the parameter values for the intersections of the loops for $L = 700\,\mathrm{km}$ as we did in Fig. 4. We see that the crosses and the plus signs flows away from the intersections as the baseline length deviates away from 700 km. The degeneracy can be thus resolved by an additional experiment with two different baseline length, where the difference of the two baseline lengths should be preferably large.

The fourth approach makes use of the second peak of appearance probability in addition to the first one [12]. The energy of the second peak is approximately only one third of that of the first peak, and we need sufficiently long baseline to make the second peak observable. We show pairs of loops for the first and the second peaks in Fig. 6 for $L = 1100\,\mathrm{km}$, where we find that the loops for the second peak are more stretched in the P-direction and overlap more significantly than the first-peak loops owing to the factor $\Pi \equiv (2n+1)\pi$ appearing in Eqs. (7) and (8). Crosses and plus signs correspond to values at the two intersections of the loops for the first peak. The points of same sign

are separated from each other on the second peak loops and the hierarchy degeneracy will be thus removed by using two peaks.

V. CONCLUSION AND DISCUSSIONS

We studied the search for the leptonic CP-violating angle δ and the neutrino mass hierarchy $\mathrm{sgn}\,\delta m^2_{31}$ by an observation of the $\nu_\mu \to \nu_\mathrm{e}$ oscillation with long baseline experiments. The energy spectrum of $\nu_\mu \to \nu_\mathrm{e}$ appearance probability gives clues to the values of these parameters, but may lead to degeneracy when the two spectra corresponding to the two different parameter values are indistinguishable. We implement the presence of degeneracy using the following criterion: the oscillation probabilities for the two parameter values are peaked at the same energy and have the same peak probability. From the viewpoint of this peak-matching condition, we examined systematically the presence of the degeneracy varying the value of δ, the sign of δm^2_{31}, and the baseline length. We have also studied how the degeneracy is resolved by a single experiment and a combination of experiments.

We have shown that the loops traced by the peak position offer intuitive view on the parameter degeneracy. A pair of disjoint loops indicate the absence of degeneracy while intersecting loops do the presence, and each of intersections corresponds to two sets of parameter values that are degenerate. Deriving analytic expressions of the loop, we systematically studied their dependence on the mass parameters, the mixing parameters, and the baseline length. We have seen that a pair of loops with different hierarchies are completely separated when the baseline is longer than the critical length, which is typically about 1000 km or longer and inversely proportional to $\sin\theta_{13}$. We cited four approaches for resolving the degeneracy by long baseline experiments: taking the baseline longer than the critical length, employing anti-neutrinos as well as neutrinos, using two or more different baseline lengths, and carrying out experiments covering more than one oscillation peaks. We went into each idea in terms of the peak loops and mentioned that the second approach using anti-neutrinos may require a high resolution to take advantage of using both neutrinos and anti-neutrinos.

The peak loops we employed have an equal significance to the trajectories in the bi-channel plots introduced in the reference [7], but simultaneously have differences from them: our plot employs only a single channel and thus can be applied to single-channel experiments to explore possibilities their possibilities; we make essential use of the oscillation peak as a representative of the spectrum over a finite energy range, while the bi-channel plot is drawn for an arbitrary fixed energy or for integrated values over an energy range at one's convenience.

We have kept the values of parameters fixed except for δ and $\mathrm{sgn}\,\delta m^2_{31}$, assuming that these values would be settled in advance of experiments. Their ambiguities may, however, persist at the time of experiments and hinder the searches [5, 6, 7, 8, 10]. We can apply the peak loop to a comprehensive understanding of effects of these ambiguities also. We leave them for future works.

Acknowledgements

The authors are grateful to Professor Joe Sato for his encouragement during this work.

[1] B. T. Cleveland *et al.*, *Astrophys. J.* **496** (1998) 505; Y. Fukuda *et al.*, *Phys. Rev. Lett.* **77** (1996) 1683; J. N. Abdurashitov *et al.*, *J. Exp. Theor. Phys.* **95** (2002) 181 [*Zh. Eksp. Teor. Fiz.* **122** (2002) 211]; W. Hampel *et al. Phys. Lett.* **B447** (1999) 127; M. Altmann *et al.*, *Phys. Lett.* **B616** (2005) 174; M. B. Smy *et al.*, *Phys. Rev.* **D69** (2004) 011104; S. N. Ahmed *et al. Phys. Rev. Lett.* **92** (2004) 181301; B. Aharmim *et al. Phys. Rev.* **C72** (2005) 055502. Y. Ashie *et al.*, *Phys. Rev. Lett.* **93** (2004) 101801; Y. Ashie *et al.*, *Phys. Rev.* **D71** (2005) 112005; M. C. Sanchez *et al.*, *Phys. Rev.* **D68** (2003) 113004; M. Ambrosio *et al.*, *Eur. Phys. J.* **C36** (2004) 323. T. Araki *et al.*, *Phys. Rev. Lett.* **94** (2005) 081801; E. Aliu *et al.*, *Phys. Rev. Lett.* **94** (2005) 081802. M. Apollonio *et al.*, *Eur. Phys. J.* **C27** (2003) 331.

[2] W. M. Yao *et al.*, *J. Phys.* **G33** (2006) 1.

[3] F. Ardellier *et al.*, [arXiv:hep-ex/0405032]; J. Cao, *Nucl. Phys. Proc. Suppl.* **155** (2006) 229; M. Aoki *et al.*, [arXiv:hep-ex/0607013].

[4] Y. Itow *et al.*, KEK report 2001-4, ICRR-report-477-2001-7, TRI-PP-01-05 [arXiv:hep-ex/0106019]. D. S. Ayres *et al.*, Fermilab-Proposal-0929 [arXiv:hep-ex/0503053].

[5] A. Cervera *et al.*, *Nucl. Phys.* **B579** (2000) 17; **B593** (2001) 731(E); M. Koike, T. Ota, and J. Sato, *Phys. Rev.* **D65** (2002) 053015; J. Burguet-Castell *et al.*, *Nucl. Phys.* **B608** (2001) 301; M. Freund, P. Huber, and M. Lindner, *Nucl. Phys.* **B615** (2001) 331; J. Pinney and O. Yasuda, *Phys. Rev.* **D64** (2001) 093008; P. Huber, M. Lindner, and W. Winter, *Nucl. Phys.* **B645** (2002) 3; H. Minakata, H. Nunokawa, and S. J. Parke, *Phys. Rev.* **D66** (2002) 093012; J. Burguet-Castell *et al.*,

Nucl. Phys. **B646** (2002) 301; P. Huber *et al.*, *Phys. Rev.* **D70** (2004) 073014; O. Mena and S. J. Parke, *Phys. Rev.* **D70** (2004) 093011; A. Donini, E. Fernandez-Martinez, and S. Rigolin, *Phys. Lett.* **B621** (2005) 276; P. Huber, M. Lindner, and W. Winter, *JHEP* **0505** (2005) 020; P. Huber, M. Maltoni, and T. Schwetz, *Phys. Rev.* **D71** (2005) 053006.

[6] Y. F. Wang *et al.*, *Phys. Rev.* **D65** (2002) 073021; M. Aoki *et al.*, *Phys. Rev.* **D67** (2003) 093004; K. Whisnant, J. M. Yang and B. L. Young, *Phys. Rev.* **D67** (2003) 013004; V. Barger, D. Marfatia, and K. Whisnant, *Phys. Lett.* **B560** (2003) 75; M. Ishitsuka *et al.*, *Phys. Rev.* **D72** (2005) 033003; K. Hagiwara, N. Okamura, and K. i. Senda, *Phys. Lett.* **B637** (2006) 266; **B641** (2006) 491(E); T. Kajita *et al.*, *Phys. Rev.* **D75** (2007) 013006.

[7] H. Minakata and H. Nunokawa, *JHEP* **0110** (2001) 001; H. Minakata, H. Nunokawa and S. J. Parke, *Phys. Lett.* **B537** (2002) 249.

[8] V. Barger, D. Marfatia, and K. Whisnant, *Phys. Rev.* **D65** (2002) 073023.

[9] M. Koike and M. Saito, STUPP-07-189 [arXiv:hep-ph/0703040] (submitted to *Phys. Rev.* **D**).

[10] M. Koike *et al.*, *Phys. Rev.* **D73** (2006) 053010.

[11] J. Arafune, M. Koike, and J. Sato, *Phys. Rev.* **D56** (1997) 3093; **D60** (1999) 119905(E); M. Koike and J. Sato, *Mod. Phys. Lett.* **A14** (1999) 1297; M. Koike and J. Sato, *Phys. Rev.* **D61** (2000) 073012; **D62** (2000) 079903(E).

[12] M. V. Diwan *et al.*, *Phys. Rev.* **D68** (2003) 012002.